Calibration of the STAR TPC:
Distortions in the Transverse Plane

J.C. Dunlop, H. Long, F. Retiere°, J.H. Thomas°, S. Trentalange and H. Wieman°*
Yale University* and Lawrence Berkeley National Laboratory°

The STAR time projection chamber[i] (TPC) sits in a uniform magnetic field and it utilizes a uniform electric field that is defined by a nearly perfect mechanical geometry. See Figure 1. The E and B field induced distortions in the transverse plane are, therefore, small, simple, and linear when compared to previous experiments and even previous generations of TPCs. None-the-less, the STAR collaboration has physics goals that demand a detailed understanding of these distortions.

One of the most demanding physic goals is to be able to distinguish positive tracks from negative tracks at high p_T. The problem is that (nearly) straight line tracks can be distorted so they acquires a random radius of curvature and they can even end up with the wrong charge sign … leading to errors in the ratio of positive to negative tracks. Another challenging problem is to be able to align independent tracks from external detectors with the tracks found in the TPC.

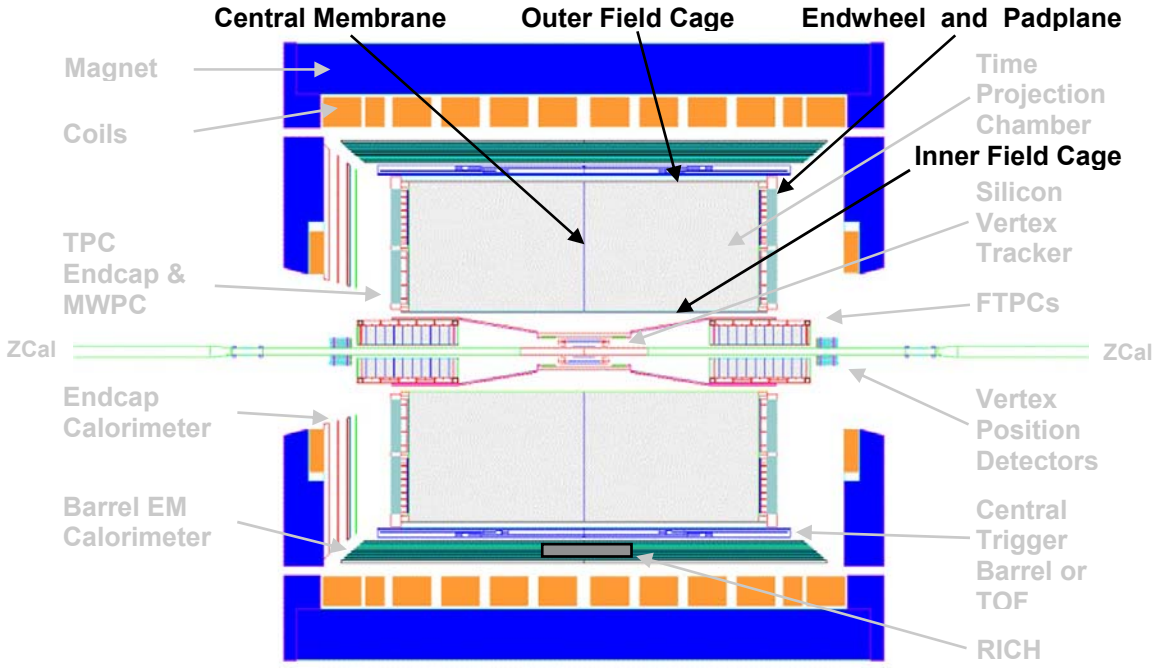

Figure 1: The STAR detector is cylindrically symmetric. The beams come from the left and the right and they collide at the middle of the detector. The detector is shown with the full suite of year 1 and year 2 detectors labeled in gray. The most important components of the TPC are labeled in black and identifying them helps us identify which calibration corrections to apply to the TPC data.

These issues are compounded when several TPC tracks are required to reconstruct a resonance or to find the V_0 associated with the complex decay topology of a short lived

particle. We might hope to take advantage of this increased complexity and increased sensitivity to calibrate the TPC if the resonances were kinematically well-defined but, unfortunately, there aren't any resonances or simple scattering reactions that we can use for calibration at RHIC. Thus, we are forced to calibrate the TPC by indirect methods.

As mentioned above, many of the distortion corrections that need to be applied to the data are due to imperfections in the electric and magnetic fields surrounding the TPC. An additional source of distortion is the mechanical miss-alignment of components such as the alignment of the inner and outer sectors of the TPC pad plane.

It is possible to completely and accurately correct for these distortions if we have a good map of the electric and magnetic fields in the TPC, and an accurate survey of the mechanical components. The usual course of action is to calculate the distortions using the Langevin equations[ii].

For example, the magnetic field induced distortions can be calculated by assuming $B_x \approx B_y << B_z$ and using equations (1) and (2).

$$\delta_x = \int \frac{-\omega\tau B_y + \omega^2\tau^2 B_x}{\left(1+\omega^2\tau^2\right) B_z} dz \qquad (1)$$

$$\delta_y = \int \frac{\omega\tau B_x + \omega^2\tau^2 B_y}{\left(1+\omega^2\tau^2\right) B_z} dz \qquad (2)$$

where δx and δy are the distortions of the tracks in the (x,y) plane as a function of (x,y,z).

The electric field induced distortion can be calculated assuming $E_x \approx E_y << E_z$ and using equations (3) and (4).

$$\delta_x = \int \frac{E_x + \omega\tau E_y}{\left(1+\omega^2\tau^2\right) E_z} dz \qquad (3)$$

$$\delta_y = \int \frac{E_y - \omega\tau E_x}{\left(1+\omega^2\tau^2\right) E_z} dz$$

where

$$\omega\tau \equiv \frac{u_z}{E_z} B_z = \frac{Drift\ Velocity}{Electric\ Field} B_z \qquad (4)$$

The drift velocity, the electric field, and the magnetic field all have signs that are important. So, for example, the electric field in STAR always points towards the central membrane of the TPC, electrons always drift away from the central membrane, and the B field can go either way. Thus, ωτ is a signed quantity and the sign depends on the direction of all of these fields. (Note that this statement disagrees with the advice given

in Blum and Rolandi (Ref. ii); they are wrong and their equations can only be used to calculate the magnitude of the distortions and not their direction or sign.)

The mathematics is precise but the mathematics depends on accurate field maps and accurate input information. Developing this information is not a simple task. The STAR detector is shown in Figure 1 and this figure is a useful pneumonic for creating a list of the required calibrations that need to be performed on the TPC data.

The list can be enumerated by surfaces:

1. Outer field cage corrections
2. Inner field cage corrections
3. Central membrane corrections
4. End-wheel and pad-plane corrections
5. Pad Row 13 corrections and other local electrostatic defects
6. Rotation and miss-alignment of sectors with respect to their ideal locations
7. Rotation of either TPC end-wheel with respect to its ideal location

and by volume:

8. Space Charge corrections due to charge in the volume of the TPC
9. Magnetic field corrections due to B fields in the volume of the TPC
10. Twist of the TPC with respect to the magnetic field axis and/or the measured map
11. General coordinate transformations

A few additional items are listed for completeness. These items affect the drift of the electrons in the Z direction but do not strongly affect the distortions in the transverse (x,y) plane.

12. Gas composition and variations in the drift velocity
13. Barometric pressure changes and variations in the drift velocity
14. Pressure variations as a function of height in the TPC
15. Temperature gradients in the TPC

Let's look at the list and make a few comments about each item as we go from top to bottom.

1. The outer field cage (OFC): The canonical assumption is that the outer OFC is a perfect cylinder and any misalignments of the OFC with respect to the rest of the detector will be attributed to the other TPC surfaces. A good example is a possible miss-alignment between the inner field cage (IFC) and the outer field cage. The difference will be attributed to the IFC, or in other words, the OFC is the reference.

The OFC can be the cause of distortions but we do not know of any at this time. Examples include sagging of the cylinder, or a shorted stripe on the field cage. We have calculated[iii] the effect of a shorted stripe on the field cage and we have a model for the perturbed electric field that it creates. The effect of a shorted stripe is big and it is a very undesirable imperfection to have in the TPC.

2. Inner field cage (IFC): The IFC can have a shorted stripe. It may also sag or it may be tipped (ie. the two ends of the cylinder may not be parallel) but we are not aware of any of these distortions in the STAR TPC.

The IFC is, however, miss-aligned with respect to the OFC and the mid-point of the IFC is not located at the same Z position as the midpoint of the OFC. The miss-alignment is approximately 0.0150 mm towards the right in Figure 1 and it results in an electric field that defocuses the tracks near the vertex and leads to a signed distance-of-closest-approach (DCA) error of approximately 0.6 mm[iv].

The electric field due to the error voltage on the IFC is:

$$E_r = \frac{4\,x\,\left|\vec{E}\right|}{L}\sum_{n=1}^{\infty}\frac{K_0(kb)\,I_1(kr)+K_1(kr)I_0(kb)}{K_0(kb)\,I_0(ka)-K_0(ka)I_0(kb)}\sin(kz)$$

And the distortion it causes is:

$$\delta_r = \frac{4\,x}{L}\sum_{n=1}^{\infty}\frac{K_0(kb)\,I_1(kr)+K_1(kr)I_0(kb)}{K_0(kb)\,I_0(ka)-K_0(ka)I_0(kb)}\;\frac{1+\cos(kz)}{k}$$

where **E** is the electric field inside the TPC, x is the amount of shift, L is the distance from the CM to one end-wheel, k = (2n-1)π/L, *a* and *b* are the radii of the inner and outer field cages respectively, and **I** and **K** are the modified Bessel functions.

The DCA error due to the IFC shift is anti-symmetric across the central membrane and it is independent of the charge density in the TPC (see figures 2 and 3). These systematic effects are important in distinguishing the shifted IFC corrections from space charge corrections which also cause a signed DCA error (see below).

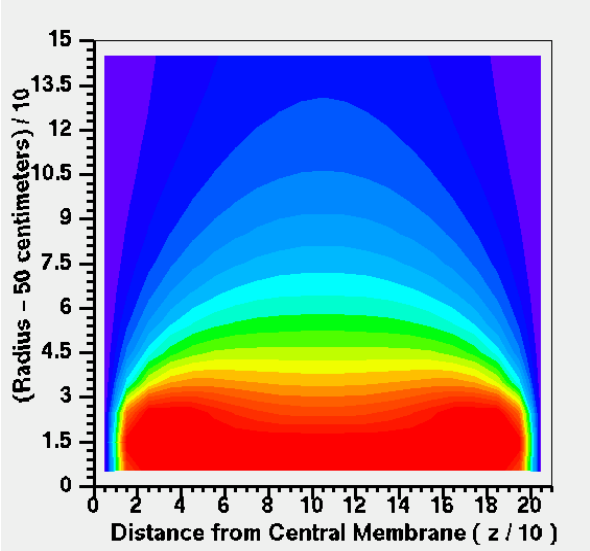

Fig. 2: The electric field in the TPC due to a shift of the IFC. One quadrant of the TPC volume is shown in (R,Z) coordinates. The magnitude of the electric field is shown as different colored contours in the figure (arbitrary units).

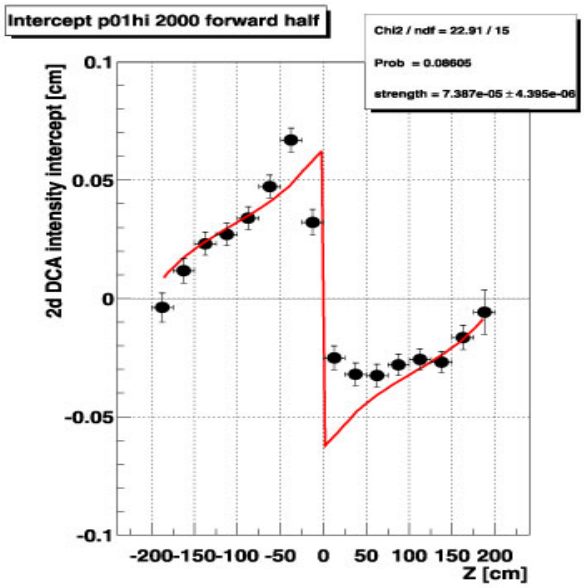

Fig. 3: The observed DCA of tracks near the vertex (points) are well described by the model (line) using a 140 μm shift of the IFC.

3. The central membrane (CM): The central membrane defines the electric field at the middle of the TPC. It was designed to be flat. It is supported at approximately 60 points around the OFC but it does not touch the IFC and is unsupported at the IFC. The CM is reinforced with an extra layer of material near the IFC and so the membrane is relatively stiff at this point. The CM can, and probably does, have shape distortions. The shape distortions lead to distortions of the electric field and the most likely scenario is that one or more of the attachment points on the OFC is not perfectly located at Z = 0. Reasonable miss-alignments are on the order of 200 – 400 μm.

The CM was surveyed from both ends of the TPC during the construction of the TPC. The survey shows that the CM is tilted from top to bottom and it looks like the bottom of the CM is pulled towards one end of the TPC by about 0.5 mm, however the two surveys do not agree with one another and the disagreement is approximately 0.5 mm. We have created an electric field map for the CM as represented by the average of the two surveys and this map is available in the STAR software library. However, the distortions produced by the CM electric field map appear to create unwanted corrections to the tracks when compared to the tracks observed with the RICH detector. This problem has not been solved.

4. The end-wheels of the TPC: The end-wheels are very complex and so many distortions are possible in this region. Fortunately, the drift volume of the TPC is very effectively defined by the CM, the OFC, the IFC, and the ground plane of wires on each read-out sector of the end-wheel. Thus, the ground planes define the most important electrostatic surface in this region.

The end-wheel was designed to be flat and therefore the ground planes associated with all 12 sectors on one end should be parallel and flat as well. However, the end-wheels are large mechanical structures (4 meters) and the mechanical tolerances on large parts are difficult to maintain. So the end-wheels were machined in two parts and the halves were bolted together; then a final cut was made on a large end-mill to flatten the sides of each end-wheel. But at the few hundred micron level, a few distortions are still possible. The two halves may define a "V" shape across the line where they are bolted together. The end-wheel can also have a bowl shape due to the elasticity of the Aluminum parts that were bolted down during the final cut on the end-mill. The two sides are parallel during the final cut but the parts could have sprung back into a curved bowl shape after the hold-down-bolts were released.

A final distortion to consider is that the end-wheels are inserted into the ends of the tube defined by the OFC. The insertion may not be perfect and therefore the end-wheel can be tipped; up-down or left-right. It is not unreasonable to think that the tipping could be 200-400 microns, overall.

The two end-wheels were surveyed during assembly of the TPC at Brookhaven National Laboratory and we have created an electric field map[v] based on the assumption that the ground planes follow the shape of the end-wheels. This map is available in the STAR software library; however the distortions produced by the end-wheel electric field map appear to disagree with the tracks locations measured with the RICH. This problem has not been solved.

5. Pad Row 13 and other sector boundary effects: Each end-wheel of the TPC is divided into 12 super-sectors and each super-sector is divided into two sub-sectors[i,vi]. The boundary between the inner and outers sub-sector is located in-between pad rows 13 and 14. There is a gap in the ground plane at this radius which is 1.6 cm wide. The resulting electrostatic distortion "sucks" electrons into the gap and the tracks are distorted in a way that depends on their direction and path.

We have calculated the electric field in the direction perpendicular to the gap at pad Row 13[vii] and it is:

$$E_y(y,z) = \frac{-\pi}{(y_{\max} - y_g)} \left[\sum_{m=0}^{N} m\ c_m\ \exp\left(\frac{-m\pi z}{(y_{\max} - y_g)} \right) \sin\left(\frac{m\pi (y - y_g)}{(y_{\max} - y_g)} \right) \right]$$

where y is the coordinate direction perpendicular to the pad rows in a local coordinate system, y_g is the center of the gap between pad rows 13 and 14, y_{max} is the maximum dimension of a hypothetical box in which the solution is calculated (usually taken to be 200 cm), z is the coordinate direction along the beam axis, m is an integer, and

$$c_0 = \frac{d\ \delta V_{eff}}{2\ (y_{\max} - y_g)} \qquad and \qquad c_{m\geq 1} = \frac{2\ \delta V_{eff}}{m\ \pi} \left[\sin\left(\frac{m\pi d}{2\,(y_{\max} - y_g)} \right) \right]$$

where d is the width of the gap in the ground plane between pad rows 13 and 14, and δV_{eff} is the effective "error" potential in the gap (difference from the nominal value as defined by the ground planes).

A map of this electric field is available in the STAR software library and the resulting distortions are calculated using equations 3 and 4. We have checked the measured distortions on a track by track basis[viii]. The maximum distortion is about 250 microns as the tracks cross over pad rows 13 and 14 and the maximum distortion is reduced to less than 50 microns after applying the corrections calculated using the electric field map derived from the model.

The distortion routines in the STAR library are symmetric in ϕ. For high precision work in the future, it may be useful to allow a ϕ dependence in the magnitude of the correction.

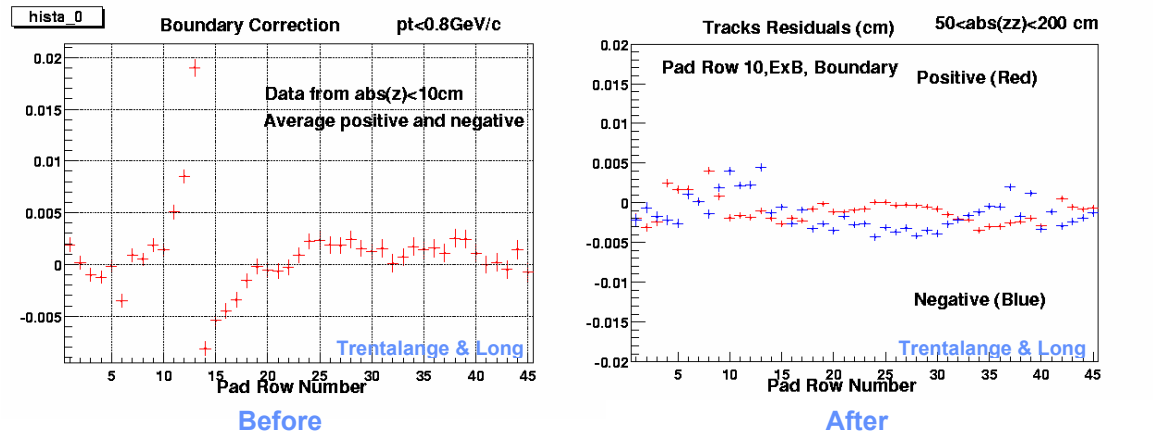

There is also a $\Delta\phi$ gap between each of the 12 super-sectors. The gap runs along the radius of the TPC and along the long edge of the sectors. The resulting electric field distortion sucks electron clusters into this gap, but since most tracks move along the radius of the TPC, this distortion is handled by taking a large fiducial cut near the sector edges. Some data is lost by the fiducial cut and it adds to the amount of track splitting for tracks that cross sector boundaries. In a perfect world, it would be better to calculate the electric field due to the $\Delta\phi$ gap and to correct the data rather than throw it away.

6. Rotation and miss-alignment of sectors: The sub-sectors that make up the readout pad-plane are independently mounted on the end-wheels of the TPC. Therefore, they can be imperfectly aligned with one another and the amount of miss-alignment is about 200 μm in random directions. The dominant effect is a coordinate shift that can, in principle, be taken out of the data. Currently, a transformation is applied to all of the data and the transformations are calibrated by analyzing individual tracks in the outer sector, alone, and then comparing the projected track with the observed track in the inner sector. The difference between these tracks is the correction that is needed for that pair of sub-sectors.

7. Rotation of the TPC end-wheels: An end-wheel is inserted into each end of the tube that defines the OFC. The orientation, in ϕ, of the end-wheels may not be perfect and so all tracks measured on one end of the TPC can be rotated with respect to the tracks on the other end. The data are easily adjusted for this coordinate transformation and the data for the transform was derived from a survey done by the BNL survey group. They found that the East end is rotated with respect to the West end by 0.43 mRad or 0.85 mm at the outer radius of the TPC. The transformation can also be checked by looking at individual tracks that cross the CM.

8. Space charge corrections in the volume of the TPC: Space charge accumulates in the volume of the TPC because of the intrinsic difference in the drift velocity for electrons and ions. The ions move 10,000 times more slowly than the electrons and so, integrated over time, there is a net positive charge in the TPC which is the result of the ionization processes that created tracks in the TPC. At year-one RHIC luminosities, the space charge contribution from tracks associated with central or minbias events is negligible but it will ***not*** be negligible at upgraded RHIC luminosities. Note, however, that the space charge from beam gas interactions and beam scraping is not negligible at any luminosity.

The radial and ϕ dependence of the space charge distributions are not known at this time. We can measure them with randomly triggered events, and we have a few runs taken with random triggers, but these data have not yet been analyzed. The radial dependence of the space charge distribution is probably a linearly decreasing function in R or perhaps 1/R**2.

The ϕ dependence of the space charge distribution has two major components. One component is due to beam gas interactions that occur far upstream of the accelerator. These tracks are traveling parallel to the beam and, presumably, are symmetric in ϕ. These tracks will deposit charge through-out the volume of the TPC. There is almost certainly a more locally generated set of tracks that deposit charge in a horizontal plane that includes the beam pipe (because the dipole magnets at RHIC bend the beam in the horizontal plane). Thus, there should be a horizontal band of charge in the volume of the TPC, too.

Our first attempt[ix] to make space charge corrections is based upon the assumption that charge is produced uniformly through-out the volume of the TPC; uniform in R and uniform in ϕ. The final space charge distribution that goes into the calculation is a triangle function, in Z, because the deposited charge drifts very slowly towards the CM and so the accumulated charge must be integrated over the mean residence time in the TPC (~1 second). Using a Green's function technique to solve Poisson's equation, the electric field due to this space charge function is:

$$E_r = \frac{-4\,C}{L} \sum_{n=1}^{\infty} -1^{n+1} \frac{I_1(kr)\left[K_0(kb)-K_0(ka)\right]+K_1(kr)\left[I_0(kb)-I_0(ka)\right]}{K_0(kb)\,I_0(ka)-K_0(ka)I_0(kb)} \frac{\sin(kL-kz)}{k^2}$$

and the distortion it causes is:

$$\delta_r = \frac{-4\,C}{L\left|\vec{E}\right|}\sum_{n=1}^{\infty} -1^{n+1}\,\frac{I_1(kr)\left[K_0(kb)-K_0(ka)\right]+K_1(kr)\left[I_0(kb)-I_0(ka)\right]}{K_0(kb)\,I_0(ka)-K_0(ka)I_0(kb)}\,\frac{1-\cos(kL-kz)}{k^3}$$

C is a fitting parameter that represents the space charge in the TPC. We assume that it is proportional to the un-triggered count rate in the central trigger barrel counters (CTB). L is the distance from the CM to an end-wheel, **E** is the electric field inside the TPC, k = nπ/L, *a* and *b* are the radii of the inner and outer field cages, respectively, and **I** and **K** are modified Bessel Functions.

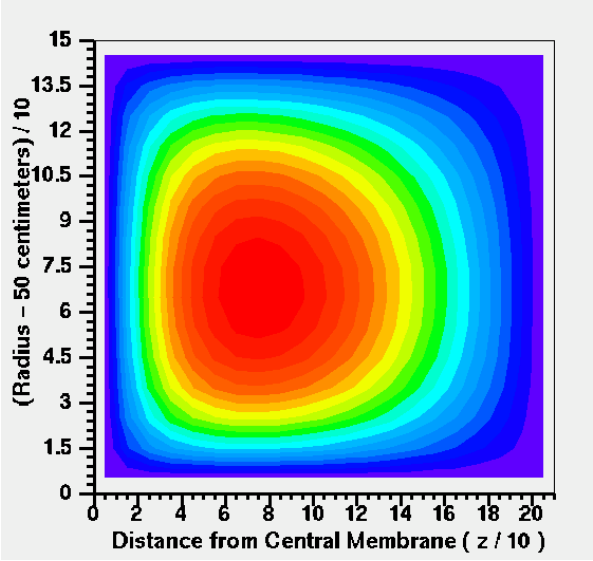

Fig. 6: The voltage pattern associated with the space charge build up in the TPC. One quadrant of the TPC is shown in (R,Z) coordinates.

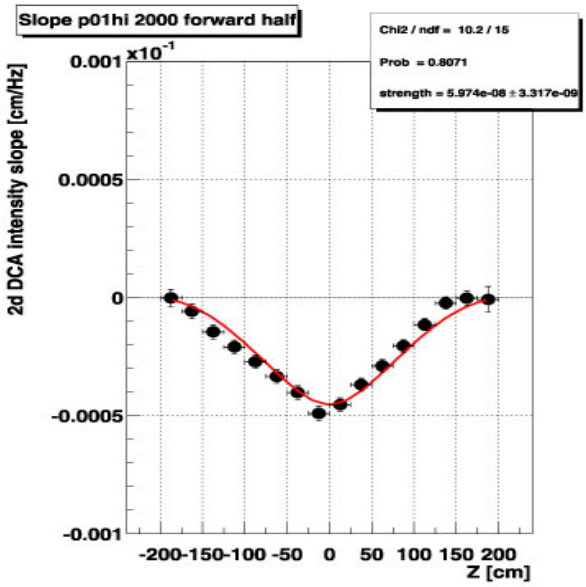

Fig. 7: The DCA of tracks near the vertex follow the trend of the model. The space charge in the TPC is estimated using track multiplicity.

The distortion causes the tracks to go "out of focus" at the event vertex but, in contrast to the IFC shift error, it is symmetric around the CM. The distortion creates a distance of closest approach error (DCA) for each track and the DCA can be measured and compared to the model. See figures six and seven.

In the future, it would be useful to have separate electric field maps for each of the various processes that can produce space charge in the TPC such as the space charge from the event, space charge from beam gas interactions (both upstream and local), and space charge that leaks through the gating grid, if any.

9. Magnetic field corrections in the volume of the TPC: Magnetic fields in the TPC affect the drift of electrons from the CM to the end-wheels. Basically, the electrons follow a path mid-way between the $\overline{E}$ and $\overline{B}$ field lines but they develop a transverse velocity due to the ($\overline{v}$ x $\overline{B}$) term in the Lorentz force equation. The transverse drift changes the sagitta of the tracks and it distorts their shape.

We are fortunate that the magnetic field in STAR is very uniform. The B_Z component of the field is 5000 ± 10 gauss and the B_R component of the field is 0 ± 40 gauss. For reference, recall that the earth's magnetic field is 0.5 to 1 gauss. Only the B_R component of the field contributes to track distortions in STAR because the E and B fields are aligned and nearly parallel.

The STAR magnet was carefully mapped before installing the TPC in the magnet. The random and systematic errors are approximately ½ gauss, respectively. The map is available in the STAR software library and the resulting distortions are calculated using equations 1 and 2. See figures 8 and 9.

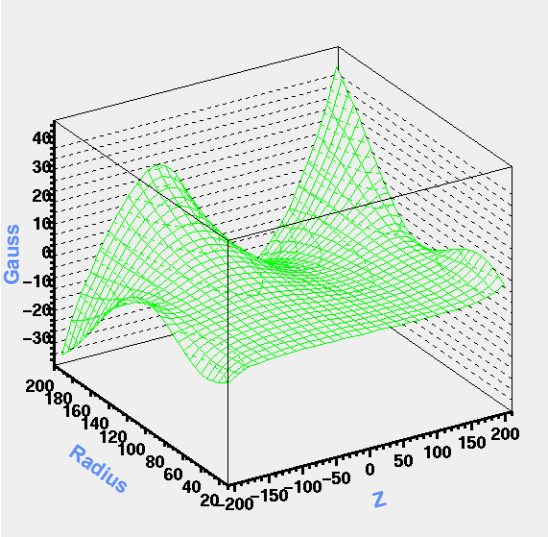

Fig. 8: The full field radial magnetic field, B_R, is plotted as a function of radius and Z. The map is cylindrically symmetric and only the fiducial volume of the TPC is shown. Note that the central membrane is at Z = 0.

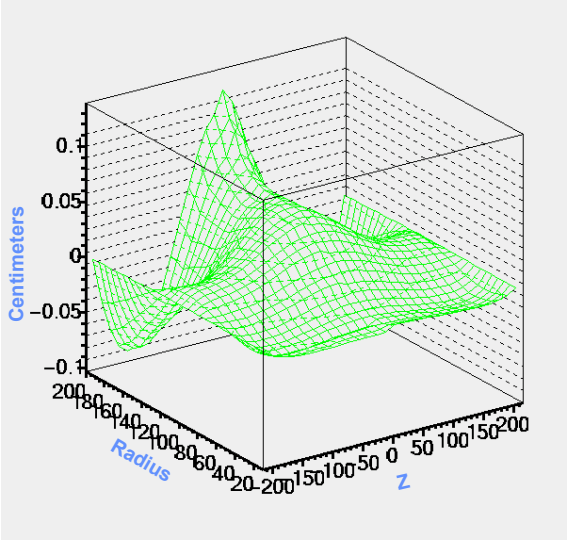

Fig 9: The figure shows the distortions due to the magnetic field map plotted in figure 8. These distortions are transverse to the direction of an infinite momentum track originating at the vertex. The range of values is ±1 mm.

The distortions due to the radial component of the magnetic field are less than 1 mm, everywhere. None-the-less, they are the biggest distortions in the TPC. The distortions are large at large radius and large near the central membrane. The distortions do not cause a big change in the primary spectra of particles but they do have a significant impact on more subtle quantities such as the position and shape of resonances reconstructed from two or more decay particles. In fact, the first application of these distortion corrections was to fix the apparent shift in the mass of the K0 and to fix an asymmetry in the Armantero's plot for the K0s. Later, the magnetic field distortions were shown to be causing an asymmetry in the yields of Λ and $\bar{\Lambda}$, especially at high p_T.

10. Twist: The magnetic field was mapped before the TPC was in the magnet. Thus, the TPC was installed afterwards and the local coordinate system for the TPC is not perfectly aligned with the coordinate system of the magnet. The TPC is twisted so that the West end is out of alignment by 0.85 mm (~35 mils) in the horizontal plane and 0.30

mm (~10 mils) in the vertical plane. This is equivalent to a 2 gauss error in the map, however it is systematic and the resulting distortions are easily removed from the data by a straightforward calculation using equations 1 and 2. Compare this 2 gauss effect to the 40 gauss shape of the radial B field in order to estimate the magnitude of the track distortions.

11. General Coordinate Transformation: The local coordinate system of the TPC is not in perfect alignment with the magnet's coordinate system. The difference between the two has been surveyed and we have already discussed how the twist of the TPC relative to the magnet can lead to distortions of the tracks and noted that these effects can be removed with great precision.

Small translations of the TPC along the x, y, or z directions (without a twist) do not cause track distortions. The STAR magnetic field is very flat on the scale of the observed translation errors and so the change in B along x, y, or z is too small to generate significant distortions. However, a general coordinate transformation from TPC local coordinates to the overall STAR coordinate system is required in order to match the tracks from different detectors.

12. Gas composition and variations in the drift velocity: All electric and magnetic field induced distortions are a function of $\omega\tau$ (see equation 4), however, $\omega\tau$ is a function of the magnetic field, the electric field, and the drift velocity of the electrons in the gas. Thus, anything that changes the drift velocity will change the magnitude of the distortions. One way to change the drift velocity is to alter the gas composition inside the TPC. Fortunately, the STAR TPC runs at the peak of the drift velocity curve and the peak is broad and flat. Thus, small changes in the gas composition are usually not significant. Large changes in gas composition are significant and this occasionally happens.

13. Barometric pressure and variations in the drift velocity: Barometric pressure changes will affect the TPC because the TPC is run at ambient pressure (plus a small differential). Pressure changes will change the drift velocity and the reduced electric field (i.e. E/P).

14. Pressure changes as a function of height in the TPC: The experts say that we should worry about the change in pressure as a function of height in the TPC. These effects are small and we have not yet found a reason to worry about this.

15. Temperature gradients in the TPC: Temperature gradients in the TPC will cause the drift velocity to change across the width and breadth of the TPC. The experts say that we should worry about this, but so far, we have not seen a physics spectrum that appears to be distorted by temperature gradients. We expect these effects to be small but more work is need in this category.

Conclusions

There are a large number of distortion corrections that can and should be applied to the data. We have attempted to rank order them by size in the following table. The rank order is an intuitive guess on our part and should only be taken as a rough guide as to the importance of each correction.

Distortion	Magnitude	Probable Error	Comments
Magnetic Field Shape	±1 mm, ±40 gauss	50 μm, ±0.5 gauss	global
Twist	±500 μm, ±2 gauss	50 μm, ±0.5 gauss	global
Space Charge	±500 μm	50 μm – 100 μm	global
IFC shift	±250 μm	50 μm	global
Pad Row 13	±250 μm	50 μm	local
Sector miss-alignments	±250 μm	50 μm	local
CM corrections	±200 μm	50 μm	global
End wheel shape	±200 μm	50 μm	global

References

[i] TPC Nim references – overall STAR TPC
[ii] Blum and Rolandi as modified by JT
[iii] Howard's reference to shorted stripe … web page
[iv] J.C. Dunlop and J. H. Thomas, "Inner Field Cage Induced Distortions in the STAR TPC", http://www.lbl.gov/nsd/annual/2001/abstracts/RNC_abstracts.html
[v] H.H. Wieman, endwheel electric field web page reference.
[vi] TPC NIM reference and electronics references – emphasize sectors and pad plane design
[vii] H.H. Wieman, personal communication. http://www.star.bnl.gov/~wieman/web2d/stripdistortion2d.htm
[viii] Long and Tretalange web page on pad row 13 distortions. Also last years LBL progress report.
[ix] J.C. Dunlop and J. H. Thomas, "Space Charge Distortions in the STAR TPC ", http://www.lbl.gov/nsd/annual/2001/abstracts/RNC_abstracts.html